Published in final edited form as:
Environ Sci Technol. 2009 March 1; 43(5): 1605–1611.

Quantum Dot Nanotoxicity Assessment Using the Zebrafish Embryo

Tisha C. King-Heiden[†,1,2], **Paige N. Wiecinski**[1], **Andrew N. Mangham**[3], **Kevin M. Metz**[‡,4], **Dorothy Nesbit**[2], **Joel A. Pedersen**[1,4], **Robert J. Hamers**[3], **Warren Heideman**[1,2], and **Richard E. Peterson**[*,1,2]

1*Molecular and Environmental Toxicology Center, University of Wisconsin, Madison WI, 53706*

2*School of Pharmacy, University of Wisconsin, Madison WI, 53706*

3*Department of Chemistry, University of Wisconsin, Madison WI, 53706*

4*Environmental Chemistry and Technology Program, University of Wisconsin, Madison WI, 53706*

Abstract

Quantum dots (QDs) hold promise for several biomedical, life sciences and photovoltaic applications. Substantial production volumes and environmental release are anticipated. QD toxicity may be intrinsic to their physicochemical properties, or result from the release of toxic components during breakdown. We hypothesized that developing zebrafish could be used to identify and distinguish these different types of toxicity. Embryos were exposed to aqueous suspensions of $CdSe_{core}$/ZnS_{shell} QDs functionalized with either poly-L-lysine or poly(ethylene glycol) terminated with methoxy, carboxylate, or amine groups. Toxicity was influenced by the QD coating, which also contributed to the QD suspension stability. At sublethal concentrations, many QD preparations produced characteristic signs of Cd toxicity that weakly correlated with metallothionein expression, indicating that QDs are only slightly degraded *in vivo*. QDs also produced distinctly different toxicity that could not be explained by Cd release. Using the zebrafish model, we were able to distinguish toxicity intrinsic to QDs from that caused by released metal ions. We conclude that developing zebrafish provide a rapid, low- cost approach for assessing structure-toxicity relationships of nanoparticles.

Introduction

Fluorescent semiconductor nanocrystals, or quantum dots (QDs), hold considerable promise in biomedical imaging, diagnostics, electronics, and photovoltaics (1,2). QDs are composed of semiconductor core (*e.g.*, CdSe, CdTe), and are often encapsulated by a shell (*e.g.*, ZnS) to enhance optical and electronic properties (3) and reduce core metal leaching (4). For many

[*]Corresponding author: School of Pharmacy, 777 Highland Ave, University of Wisconsin, Madison WI 53705, repeterson@pharmacy.wisc.edu
Author e-mail addresses: king-hei.tish@uwlax.edu, pwiecinski@wisc.edu, anmangham@wisc.edu, kmetz@albion.edu, djnesbit@wisc.edu, japedersen@soils.wisc.edu, rjhamers@wisc.edu, wheidema@facstaff.wisc.edu
[†]Present address: Biology Department, University of Wisconsin, LaCrosse, WI
[‡]Present address: Chemistry Department, Albion College, Albion, MI

Supporting Information Available
Tables and figures describing Cd body burden correlations with toxicity scores and MT expression; effects of QD and $CdCl_2$ exposure on growth and spinal malformation; and Se toxicity are available free of charge via the Internet at http://www.pubs.acs.org.

BRIEF. The embryonic zebrafish model allowed toxicity intrinsic to $CdSe_{core}/ZnS_{shell}$ quantum dots to be distinguished from that caused by released metal ions.

applications, QDs are coated with organic molecules to increase dispersibility in water and to direct them to biological targets (1,5,6).

Recent advances allow large-quantity production of water-soluble QDs. Given their wide range of applications, substantial production volumes of QDs are envisioned (7,8); entry of QDs and their by-products into waterways is likely, potentially posing risks to aquatic biota. Estimated environmental residence times for QDs range from months to years (7). Most currently produced QDs are heavy metal chalcogenides (e.g., CdSe, PbS) and may constitute a hazard to wildlife and humans due to their nanoscale properties and toxic metal release.

Initial reports suggested dihydrolipoic acid-capped $CdSe_{core}/ZnS_{shell}$ QDs lacked toxicity toward mammalian (HeLa) and slime mold (AX2) cells (9); however, subsequent studies on surface-coated QDs demonstrated toxicity in various cell lines (4,7). Because QD cores generally contain toxic elements, QD cytotoxicity may result from metals leaching into solution. Some QDs may also catalyze reactive oxygen species production leading to oxidative stress (10). Evidence exists that surface modifications affecting properties such as net charge contribute to QD cytotoxicity (4,11,12).

The potential toxicity of engineered nanomaterials to aquatic organisms is poorly understood. The zebrafish (*Danio rerio*) embryo has emerged as a valuable vertebrate model for assessing developmental toxicity (13,14), and results obtained with zebrafish have relevance to human health and feral fish populations. Our objective was to use this model to identify the types of toxicity produced by CdSe QDs. We hypothesized that QDs would produce toxicity by more than one mechanism: toxicity due to Cd^{2+} release, and toxicity associated with QD nanoscale properties. Further, we hypothesized that zebrafish could be used to discriminate between toxic effects caused by Cd^{2+} and possibly unique effects associated with the QDs and their surface ligands. We used dose-response experiments to determine the toxic potency of QDs with different surface properties. Since Cd^{2+} produces a set of characteristic toxic responses in zebrafish larvae, these responses, along with metallothionein (MT) induction (an indicator of metal ion exposure) were used to detect toxicity due to Cd^{2+}. MT expression was also used to estimate Cd^{2+} release from QDs after their absorption by zebrafish.

Experimental Section

Chemicals

Chemicals used, suppliers and purities are described in Supporting Information (SI).

Quantum Dot Synthesis

$CdSe_{core}/ZnS_{shell}$ QDs were synthesized as previously described (15) and functionalized with poly-L-lysine (PLL), methoxy-terminated PEG_{350}-thiol (PEG_{350}- OCH_3), or PEG_{5000}-thiol terminated with carboxylate, methoxy or amine functional groups (*i.e.*, PEG_{5000}-COO^-, PEG_{5000}–OCH_3, PEG_{5000}–NH_3). These coatings were selected to examine the extent to which ligand chain length and terminal functional group affected uptake and toxicity. Further details are provided in the SI.

QD Characterization

Methods for calculating expected QD core diameters are provided in the SI. QD core diameter, hydrodynamic diameter (d_h) and ζ-potential were determined in stock solutions and in zebrafish embryo media (58 mM $CaCl_2$, 0.7 mM KCl, 0.4 mM $MgSO_4 \cdot 7H_2O$, 0.6 mM $Ca(NO_3)_2 \cdot 4H_2O$, 0.5 mM HEPES, pH 7; ionic strength (I) = 0.18 M; 24-h exposure at 28°C). QD core diameter and number concentration were estimated by UV-Visible spectrophotometry (Shimadzu PC-2401) (16). A blue shift in the first exciton peak position signals a decrease in

CdSe core diameter, while declines in QD concentrations are indicated by diminished first exciton peak absorbance (16,17). Inductively coupled plasma-optical emission spectroscopy (ICP-OES) was used to measure Cd release from QDs.

QDs were diluted in embryo media or ddH_2O ("stock" control) and incubated under experimental conditions, after which UV-Visible absorption spectra were collected. QD d_h were determined by dynamic light scattering (DLS; Malvern Zetasizer Nano-ZS). QD number distributions d_h were estimated using the ZnS refractive index (2.3). QD electrophoretic mobilities were determined by phase analysis light-scattering and converted to ζ-potentials (Smoluchowski equation). To determine dissolved Cd concentrations, nanoparticle solutions were filtered using Millipore Centricon centrifugal concentrators with regenerated cellulose membranes (10 kDa MWCO); filtrates and retentates were diluted to 10 mL with ddH_2O, and pH was adjusted to <2 with HNO_3. Cadmium concentrations were determined by ICP-OES (average of peak intensities at 214.439, 226.502, and 228.802 nm).

Zebrafish Exposures

QD exposure suspensions were prepared in embryo media without sonication and within two days of synthesis. Concentrations of 0, 0.2-200 μM-Cd equivalents (*i.e.*, total Cd per unit volume QD suspension) were used. $CdCl_2$ and $SeCl_4$ dosing solutions were prepared in embryo media at concentrations of 0-1600 μM. Exposures to $ZnCl_2$ and each ligand employed were conducted at concentrations ranging from zero to the concentration that would result from complete dissolution of shell and release of the organic coating.

Fertilized eggs were collected from AB strain zebrafish and distributed in 96-well cell culture plates (one embryo/well); embryos were raised at 28°C (18). Triplicate experiments (n = 12 embryos/treatment/replicate) were conducted to determine dose-dependent effects of QDs, ligands, $CdCl_2$, $ZnCl_2$, and $SeCl_4$. Embryos were exposed to graded concentrations of all materials beginning at the sphere stage (4-6 hours post fertilization, hpf), and dosing solutions (100 μL) were renewed every 24 h through 5 days post fertilization (dpf). Embryos/larvae were screened daily and scored for survival, alterations in morphology and endpoints of toxicity (19). Embryos were scored for severity of toxicity [0 = normal, no toxic response; 1 = minor, one or two toxic endpoints; 2 = moderate, two or three toxic endpoints; 3 = severe, more than three toxic endpoints; 4 = dead]. Toxic endpoints included bent spine; ocular, submaxillary, pericardial, or yolk sac edema; reduced growth; malformed yolk sac; tail fin malformation, and opaque head, yolk, or body tissue (apparent necrosis).

Toxic responses were evaluated following 120-h exposure to a QD concentration (2 μM Cd-equivalents) that produced endpoints of toxicity with minimal mortality. Four larvae from each replicate (n = 12) were immobilized in 3% methylcellulose and photographed live (2.5x) in lateral orientation. Photomicrographs of larvae were analyzed to determine body length and degree of axial curvature (bent spine). Incidence of pericardial, yolk sac, cranial, or submaxillary edema; tail fin malformation; and opaque tissue were determined.

Cd Body Burden Determination

Due to the low QD concentrations used and possible decreases in luminescence efficiency due to surface quenching (20). QDs could not be observed via *in vivo* optical detection. Cd accumulation in developing embryos was assessed by determining total Cd body burden using graphite-furnace atomic-absorption spectrophotometry (GFAA) (21). Following 120-h exposure to embryo media (control), QDs, or $CdCl_2$, larvae (10/replicate) were euthanized with 3-aminobenzoic acid ethyl ester, rinsed thrice, and transferred to preweighed microcentrifuge tubes. Excess water was removed, and larvae wet weights were determined. Tissues from whole larvae were digested for 24 h in 1 mL 5% HNO_3 at 60°C. Samples were diluted 1:3 with

ddH$_2$O, and analyzed by GFAA (Perkin Elmer 3030) using 20-μL aliquots diluted 1:2 with 1 mg mL^{-1} Mg(NO$_3$)$_2$ in 5% HNO$_3$ as a matrix modifier. Three replicates were analyzed per dose. Reported Cd concentrations were background corrected by subtracting the Cd concentration of unexposed control fish (~6 ng·g^{-1}, near detection limit) (21).

Gene Expression

Metallothioneins are induced by exposure to metals such as Cd^{2+}, and influence their transport and storage within organisms. MT expression was used as a biomarker of Cd^{2+} exposure. Relative MT mRNA abundance was determined at 120 hours post dosing (hpd) with QDs or $CdCl_2$ as an indicator of internal exposure to Cd^{2+}. Total RNA was isolated from pools of five larvae using QIAGEN RNeasy Mini kit, and first strand cDNA was synthesized using SuperScript™ III RT-PCR kit (Stratagene). MT and β-actin transcripts were quantified using LightCycler FastStart DNA Master SYBR Green I kit with gene-specific primers (β-actin forward: AAGCAGGAGTACGATGAGTC; β-actin reverse: TGGAGTCCTCAGATGCATTG; MT forward: CACCTGCAAGTGCACCAA; MT reverse: AACATTCATGCGATGGAAAA). MT mRNA abundance was normalized to β-actin. Three replicate experiments were performed and fold-changes averaged.

Statistical Analysis

Cumulative toxicity scores for each 24-h time point were averaged and used as a metric of overall toxicity, including mortality and sublethal toxicity. LC_{50} values were calculated by probit analysis (USEPA Probit Analysis Program, Ver 1.5) from 120-hpd mortality data. Data were evaluated for homoscedasticity (Leven Median test) and by one-way ANOVA. Pair-wise multiple comparisons were conducted using Tukey's test. Fisher's Exact Probability test was used to determine whether treated larvae showed increased incidence of endpoints of toxicity. Level of significance for all analyses was $p < 0.05$.

Results and Discussion

QD Suspension Stability

Assessment of nanoparticle aggregation and stability under exposure conditions is necessary to correctly interpret biological effects. Nanoparticle aggregation influences uptake by cells and whole organisms (26), and variables such as the surface ligands and the solution composition influence nanoparticle suspension stability (22,23). Furthermore, if nanoparticles dissolve in exposure media, toxic responses could be due to dissolved constituents.

We characterized QD suspension stability using DLS, electrophoretic light scattering, and Cd release by ICP-OES under exposure conditions. Table 1 shows calculated QD diameters and measured number-average hydrodynamic diameters ($d_{h,n}$). Except for $CdSe_{core}/ZnS_{shell}$-PLL QDs, $d_{h,n}$ were similar to those expected for single particles, indicating little aggregation in ddH$_2$O. QD $d_{h,n}$ values differed little in embryo medium, although $CdSe_{core}/ZnS_{shell}$-PEG_{350}-OCH_3 QDs aggregated severely ($d_{h,n}$ 85x larger than calculated value). $CdSe_{core}/ZnS_{shell}$-PLL QDs remained aggregated in embryo medium ($d_{h,n}$ 42x larger than calculated value). In embryo medium, aggregated QDs exhibited positive ζ-potentials, while those showing no to limited aggregation had relatively small negative ζ-potentials.

First exciton peak position in UV-Visible absorbance spectra of QD suspensions did not change under experimental conditions, indicating no detectable change in core diameter (16). For most QDs, ICP-OES results indicated minimal Cd release (< 5% of total Cd) under experimental conditions. However, $CdSe_{core}/ZnS_{shell}$-PLL and $CdSe_{core}/ZnS_{shell}$-PEG_{5000}-NH_2 QDs released 19 and 14% of their total Cd, suggesting a moderate degree of degradation under experimental conditions. Maximum possible Cd released under experimental conditions (*i.e.*,

200 μM Cd-eq of QDs) is indicated in Table 1. These Cd levels, while insufficient to induce mortality, may contribute to sublethal endpoints of toxicity.

Quantum Dot Toxicity

We conducted dose-response experiments to assess potency of different QD formulations and expressed LC_{50} values two ways: (1) QD particle number per 100 μL, and (2) total Cd in QDs available for release into solution (Cd-equivalents) per unit volume (Table 1). QDs functionalized with PEG_{350}-OCH_3 showed low potency. PLL-wrapped QDs were considerably more potent than those functionalized with PEG ligands. With one exception, QDs produced mortality to zebrafish larvae at concentrations substantially lower than for $CdCl_2$ (Table 1). Therefore, QDs were more potent in causing mortality than an equivalent amount of Cd^{2+}. This suggests that QDs are either more potent than dissolved Cd^{2+}, accumulate to a larger extent than Cd^{2+} in larvae, or both. We address each possibility below.

In vitro studies suggest that exposure to Cd released from QDs is the primary determinant of $CdSe_{core}/ZnS_{shell}$ QD toxicity (4,7). However, most QDs in our study did not release substantial amounts of Cd to the exposure medium. Cd released into exposure medium by $CdSe_{core}/ZnS_{shell}$- PLL and -PEG_{5000}-NH_2 QDs may have been taken up by embryos and induce sublethal toxicity. However, despite insignificant *ex vivo* degradation in most cases, *in vivo* QD degradation may expose embryos to Cd. This would be expected to produce endpoints of Cd toxicity in zebrafish embryos exposed to sublethal QD concentrations.

To gain insight into potential mechanisms of QD toxicity, we compared sublethal toxic effects following exposure to a single concentration of $CdCl_2$ (20 μM Cd) or QDs (2 μM Cd-eq) that induced equivalent mortality (3-6%). In zebrafish, Cd induces dose- and age-dependent endpoints of sublethal toxicity including reduced growth; ocular, pericardial, submandibular and yolk sac edema (swelling), and increased axial curvature (bent spine) (24,25) (Figures 1, S1). Larvae exposed to $CdSe_{core}/ZnS_{shell}$-PEG_{5000} QDs showed endpoints of Cd toxicity, as well as endpoints unrelated to Cd exposure, including apparent necrosis, yolk sac malformation, and malformed tail (Figure 1). We observed no endpoints of sublethal toxicity in embryos exposed to $CdSe_{core}/ZnS_{shell}$-PLL and $CdSe_{core}/ZnS_{shell}$-PEG_{350}-OCH_3 QDs at the concentrations examined.

QD Uptake and Cadmium Accumulation

We measured Cd body burden in larvae exposed to 0, and 0.2-20 μM Cd-eq of QDs to assess QD and Cd accumulation following 120-h exposure. At these concentrations, the amount of Cd released from QDs (< 4 μM Cd) is not sufficient to significantly contribute to total Cd body burden, indicating that Cd accumulation primarily reflects uptake of intact QDs. Cd body burden provides a measure of Cd accumulation (*i.e.*, uptake minus depuration assuming similar growth dilution across treatments), but yields no information on *in vivo* QD degradation. Larvae exposed to QDs contained measurable Cd body burdens; however, only those exposed to ≥ 2 μM Cd-eq of $CdSe_{core}/ZnS_{shell}$-PEG_{5000} QDs and 20 μM Cd-eq of $CdSe_{core}/ZnS_{shell}$-PLL QDs contained substantial Cd body burdens (Figure 2A). Zebrafish exposed to $CdSe_{core}/ZnS_{shell}$-PEG_{350}-OCH_3 and $CdSe_{core}/ZnS_{shell}$-PLL QDs had lower Cd body burdens relative to those exposed to other QDs or $CdCl_2$. As expected, Cd body burdens in embryos exposed for 120 h to QDs or $CdCl_2$ correlated with mean toxicity scores ($R^2 = 0.51$, $p < 0.01$; Table S1 contains individual correlations).

The $d_{h,n}$ of QDs and their aggregates influenced total Cd body burden and toxicity. QDs forming relatively large aggregates in embryo medium ($d_{h,n}$ = 382-600 nm) did not induce toxicity. Large aggregate size hindered QD uptake; $d_{h,n}$ was negatively correlated with QD accumulation ($R^2 = 0.67$, $p = 0.01$). Prior to hatching, the chorion, an acellular egg envelope

surrounding the embryo, likely restricted QD uptake. The zebrafish chorion possess 500- to 700- nm diameter pores between the vitelline membrane and syncytial layer (26) which should restrict QD passage. For example. 200- to 300-nm polymeric micelles are not taken up by zebrafish larvae until after hatching when the chorion is shed (27). Hatched larvae likely absorbed QDs intact across skin and gill epithelium (28).

Our results do not distinguish between lower bioavailability or more efficient elimination of $CdSe_{core}/ZnS_{shell}$-PLL and -PEG_{350}-OCH_3 QDs relative to those with smaller $d_{h,n}$. Bioaccumulation and elimination rates are important parameters in QD toxicokinetics and merit examination. Further, the extent to which QD aggregation state was preserved in larvae after uptake was not determined. Effects of physicochemical properties and $d_{h,n}$ on QD uptake, distribution and elimination warrant further investigation.

Metallothionein Expression

Cd body burdens do not provide direct information on *in vivo* QD degradation. We measured MT expression as a marker of internal Cd^{2+} exposure, thus providing indirect information on *in vivo* QD degradation. Consistent with previous findings (29), MT expression correlated with $CdCl_2$ exposure concentrations ($R^2 = 0.90$, $p < 0.001$, Figure 2B). Embryos exposed to QDs also showed a dose-dependent increase in MT expression ($R^2 = 0.42$, $p < 0.01$; Figure 2B) suggesting that QDs degraded at least partially *in vivo*. When assessed individually, QDs that aggregated less in solution and induced toxicity resembling Cd^{2+} showed stronger relationships between Cd body burden and MT expression (Table S1).

Some studies suggest that ZnS shell and surface ligands protect QDs from degradation *in vivo* (30,31). While nanoparticles with high molecular mass ligands are less prone to degradation, even slow degradation *in vivo* could allow metals release directly in zebrafish (5,32). Indeed, exposure of $CdSe_{core}/ZnS_{shell}$ QDs functionalized with PEG_{350}-OCH_3 and PEG_{5000}-OCH_3, to simulated gastrointestinal conditions showed degradation, releasing Cd^{2+} (33). MT likely contributes to ZnS shell degradation (34). In the present study, partial *in vivo* QD degradation may explain their Cd-like toxicity and MT induction. However, correlations between MT expression and $CdCl_2$ or QD exposure differed significantly (Table S1), indicating that QDs did not completely degrade *in vivo* and that some toxicity was unrelated to Cd^{2+} release.

Contribution of Components Other than Cd to QD Toxicity

Except for $CdSe_{core}/ZnS_{shell}$- PLL and -PEG_{350}-OCH_3 QDs, QDs used in this study caused some endpoints of toxicity similar to Cd; yet these QDs were more potent than Cd. Also, larvae exposed to $CdSe_{core}/ZnS_{shell}$- PEG_{5000} QDs exhibited additional endpoints of toxicity that differed from those of Cd including yolk malformation (yolk not absorbed by 5 dpf and appeared opaque), opaque tissue in areas of head and body (possible necrosis), and tail malformations (Figure 1A, B). Although not quantified, some larvae displayed malformed (stretched) hearts and a slower heart rate. These observations suggest that factors in addition to Cd^{2+} exposure contributed to QD toxicity.

Selenium—Some endpoints of toxicity induced by $CdSe_{core}/ZnS_{shell}$-PEG_{5000} QDs resembled Se toxicity in fishes (35), particularly heart, yolk sac, and tail malformations. However, mortality or sublethal effects were not apparent upon larvae exposure to Se concentrations that would occur if all Se was released from QDs (SeO^{2-}_4 expected under experimental conditions). Larvae had to be exposed to much higher Se concentrations ($\geq$ 200 μM) before they exhibited toxicity (*i.e.*, pericardial and yolk sac edema, yolk sac and tail malformation) similar to that caused by exposure to 2 μM Cd-equivalents of QDs (Figure S2).

Zinc—Exposure to zinc concentrations equivalent to those resulting from complete dissolution of the ZnS QD shell (0-8 μM as $ZnCl_2$) also did not cause toxicity in zebrafish embryos. Therefore, Zn was not believed to contribute to QD toxicity.

Nanoscale Properties of QDs and Oxidative Stress—The ability of QDs to efficiently transfer energy to acceptor molecules (6,36) suggests that they could promote reactive oxygen species (ROS) production *in vivo*, inducing oxidative stress leading to cell damage (10,37). Co-exposure of zebrafish embryos to QDs and reduced glutathione (GSH) provided preliminary evidence that oxidative stress may contribute to QD toxicity (38), but results were inconsistent. Co-exposure to 100 μM GSH increased LC_{50} values for $CdCl_2$ and all QDs except the $CdSe_{core}/ZnS_{shell}$ PEG_{5000}-COO^- QDs. GSH reversed non-cadmium-like toxic effects (e.g., yolk sac and tail malformations), and rescued sublethal, cadmium-like, toxic effects (e.g., altered body angle and ocular edema). Cadmium toxicity is associated with oxidative stress; therefore, information on the extent of *in vivo* QD degradation, increase in ROS production, and reduction of toxicity by co-exposure to radical scavengers are needed to determine the extent that oxidative stress contributes to QD toxicity, and whether nanoscale QD properties and/or Cd^{2+} released from QDs triggers oxidative stress.

Organic Coatings—The nature of organic coatings, in particular their net charge, may influence QD toxicity (11,39). Our results partially support this assertion via organic coating-dependent differences in developmental toxicity and the extent of QD aggregation in solution; however, we observed no direct correlation between toxicity and net QD charge.

PLL-wrapped QDs were highly toxic to zebrafish larvae, due in part to the poly-L-lysine itself. Lethality increased as PLL-QD concentrations exceeded 20 μM Cd-equivalents (Figure 3A). Studies in cell culture and mammals show PLL toxicity increases with molecular mass such that PLL > 35,000 Da is toxic (40,41). Furthermore, exposure of rainbow trout (*Oncorhynchus mykiss*) to 100,000-Da PLL altered gill membrane permeability (42). In the present study, QDs were wrapped with lower molecular mass (10,000-15,000 Da) poly-L-lysine. Nevertheless zebrafish larvae exposed to high PLL concentrations showed increased mortality at 24 hpd possibly due to altered cell permeability. Surviving embryos were 6-10% smaller than unexposed controls, but exhibited no other signs of toxicity (Figure 3B). PLL-toxicity explains the high mortality induced by the $CdSe_{core}/ZnS_{shell}$-PLL QDs despite the relatively low Cd body burden. These results illustrate the importance of not only selecting biologically benign organic coatings in designing engineered nanomaterials, but evaluating the toxicity of all QD components in a whole animal screen with human health and environmental relevance.

To further examine effect of surface chemistry on toxicity, we chose PEG, which is considered biologically inert, varying in either chain length (PEG_{350} or PEG_{5000}) or terminal functional group (–OCH_3, –COO^-, or –NH_2). Varying the terminal functional group allowed comparison of negatively charged (-COO^-) versus neutral (-OCH_3, NH_2) ligands. All PEG_{5000}- coated QDs, regardless of PEG terminal functional group, exhibited negative ζ-potentials (Table 1). With exception of PEG_{5000}-COO^-, this cannot be explained by ligand charge, but may be due to intercalation of excess PEG-thiolate. PEG_{350}–OCH_3, and PEG_{5000}-COO^-, –OCH_3 and –NH_3 were not themselves toxic; however, most QDs functionalized with these benign polymers were toxic to zebrafish embryos. LC_{50} values did not differ among PEG_{5000} QDs ($p > 0.05$). Cumulative toxicity scores suggest PEG_{5000}-OCH_3 QDs were less toxic than other PEG_{5000} QDs (Figure 3C). PEG_{5000}-OCH_3 QD-exposed larvae lacked tail malformation, had less severe yolk malformation, and had less opaque head and body tissue/necrosis (Figure 1). Several studies suggest that the terminal functional group of QD ligands influences tissue distribution (7). Because PEG_{5000}-OCH_3-coated QDs were not less bioavailable to larvae (Figure 2), we hypothesize that surface chemistry influenced tissue distribution, accounting for differences in potency and endpoints of toxicity.

Implications for Zebrafish Use in Nanomaterials Toxicity Assessment

This study demonstrates the utility of zebrafish larvae as a model for assessing potential risks of nanomaterial exposure to aquatic vertebrates. Zebrafish embryos are easier and less expensive to maintain than mammalian cell cultures, yet provide a richer repertoire of responses that can model factors influencing toxicity in natural ecosystems. These include barriers to particle absorption and distribution, and multiple cell types that provide different qualitative and quantitative responses. In addition to more accurately mirroring factors affecting toxicity in natural ecosystems, nanoparticle-induced responses in developing zebrafish provide vital clues about *in vivo* mechanisms of toxicity. We found that zebrafish larvae showed clear signs of Cd toxicity. However, nanoparticles were even more potent and produced endpoints of toxicity distinct from that of Cd^{2+}. Moreover, by using MT gene induction as an indicator of Cd^{2+} release, we were able to detect breakdown of QDs after absorption by the larvae. We expect that the versatility of developing zebrafish in producing different morphological and biochemical responses will make them extremely useful for characterizing biological responses to QDs and other nanoparticles.

Supplementary Material

Refer to Web version on PubMed Central for supplementary material.

Acknowledgement

We thank Jackie Bastyr-Cooper for ICP-OES analysis and Nikita Taylor for laboratory assistance. This work was supported by NSF award DMR-0425880. NIEHS Postdoctoral Training Grant T32 ES007015 (Contribution # 373) supported PNW and TCK. TCK was also supported by NIEHS NRSA T32 ES016714-01. Article contents are sole responsibility of the authors and do not represent official views of the sponsors.

Literature Cited

(1). Michalet X, Pinaud FF, Bentolila LA, Tsay JM, Doose S, Li JJ, Sundaresan G, Wu AM, Gambhir SS, Weiss S. Quantum dots for live cells, *in vivo* imaging, and diagnostics. Science 2005;307:538–544. [PubMed: 15681376]

(2). Gratzel M. Photovoltaic and photoelectrochemical conversion of solar energy. Philos. Transact. A Math. Phys. Eng Sci 2007;365:993–1005. [PubMed: 17272237]

(3). Nirmal M, Brus L. Luminescence photophysics in semiconductor nanocrystals. Acc. Chem. Res 1999;32:407–414.

(4). Derfus AM, Chan WCW, Bhatia SN. Probing the cytotoxicity of semiconductor quantum dots. Nano Lett 2004:11–18.

(5). Akerman ME, Chan WC, Laakkonen P, Bhatia SN, Ruoslahti E. Nanocrystal targeting *in vivo*. Proc. Natl. Acad. Sci U. S. A 2002;99:12617–12621. [PubMed: 12235356]

(6). Medintz IL, Uyeda HT, Goldman ER, Mattoussi H. Quantum dot bioconjugates for imaging, labelling and sensing. Nat. Mater 2005;4:435–446. [PubMed: 15928695]

(7). Hardman R. A toxicologic review of quantum dots: toxicity depends on physicochemical and environmental factors. Environ. Health Perspect 2006;114:165–172. [PubMed: 16451849]

(8). Aitken RJ, Chaudhry MQ, Boxall AB, Hull M. Manufacture and use of nanomaterials: current status in the UK and global trends. Occup. Med. (Lond) 2006;56:300–306. [PubMed: 16868127]

(9). Jaiswal JK, Mattoussi H, Mauro JM, Simon SM. Long-term multiple color imaging of live cells using quantum dot bioconjugates. Nat. Biotechnol 2003;21:47–51. [PubMed: 12459736]

(10). Lovric J, Cho SJ, Winnik FM, Maysinger D. Unmodified cadmium telluride quantum dots induce reactive oxygen species formation leading to multiple organelle damage and cell death. Chem Biol 2005;12:1227–1234. [PubMed: 16298302]

(11). Guo G, Liu W, Liang J, He Z, Xu H, Yang X. Probing the cytotoxicity of CdSe quantum dots with surface modification. Mater. Lett, 2007;61:1641–1644.

(12). Ryman-Rasmussen JP, Riviere JE, Monteiro-Riviere NA. Surface coatings determine cytotoxicity and irritation potential of quantum dot nanoparticles in epidermal keratinocytes. J. Invest. Dermatol 2007;127:143–153. [PubMed: 16902417]

(13). Hill AJ, Teraoka H, Heideman W, Peterson RE. Zebrafish as a model vertebrate for investigating chemical toxicity. Toxicol Sci 2005;86:6–19. [PubMed: 15703261]

(14). Spitsbergen JM, Kent ML. The state of the art of the zebrafish model for toxicology and toxicologic pathology research--advantages and current limitations. Toxicol. Pathol 2003;31(Suppl):62–87. [PubMed: 12597434]

(15). Huang GW, Chen CY, Wu KC, Ahmed MO, Chou PT. One-pot synthesis and characterization of high-quality CdSe/ZnX (X = S, Se) nanocrystals via the CdO precursor. J. Crystal Growth 2004;265:250–259.

(16). Yu WW, Qu LH, Guo WZ, Peng XG. Experimental determination of the extiction coeeficeint of cdte, cdse, and cds nanocrystals. Chem. Mater. 2003;15:2854–2860.

(17). Peng X, Wickham J, Alivisatos A. Kinetics of II-VI and III-V colloidal semiconductor nanocrystal growth: “Focusing” of size distributions. J. Am. Chem Soc 1998;120:5343–5344.

(18). Westerfield M, Doerry E, Kirkpatrick AE, Driever W, Douglas SA. An on-line database for zebrafish development and genetics research. Sem. Cell Dev. Biol 1997;8:477–488.

(19). Heiden TC, Dengler E, Kao WJ, Heideman W, Peterson RE. Developmental toxicity of low generation PAMAM dendrimers in zebrafish. Toxicol. Appl. Pharmacol 2007;225:70–79. [PubMed: 17764713]

(20). Breus V, Heyes CD, Nienhaus GU. Quenching of CdSe-ZnS core-shell quantum dot luminescence by water-soluble thiolated ligands. J. Phys. Chem. C 2007;111:18589–18594.

(21). Matz CJ, Treble RG, Krone PH. Accumulation and elimination of cadmium in larval stage zebrafish following acute exposure. Ecotoxicol. Environ Saf 2007;66:44–48. [PubMed: 16376426]

(22). Dutta D, Sundaram SK, Teeguarden JG, Riley BJ, Fifield LS, Jacobs JM, Addleman SR, Kaysen GA, Moudgil BM, Weber TJ. Adsorbed proteins influence the biological activity and molecular targeting of nanomaterials. Toxicol Sci 2007;100:303–315. [PubMed: 17709331]

(23). Teeguarden JG, Hinderliter PM, Orr G, Thrall BD, Pounds JG. Particokinetics *in vitro*: dosimetry considerations for in vitro nanoparticle toxicity assessments. Toxicol Sci 2007;95:300–312. [PubMed: 17098817]

(24). Blechinger SR, Warren JT Jr. Kuwada JY, Krone PH. Developmental toxicology of cadmium in living embryos of a stable transgenic zebrafish line. Environ. Health Perspect 2002;110:1041–1046. [PubMed: 12361930]

(25). Hen Chow ES, Cheng SH. Cadmium affects muscle type development and axon growth in zebrafish embryonic somitogenesis. Toxicol. Sci 2003;73:149–159. [PubMed: 12700413]

(26). Rawson DM, Zhang T, Kalicharan D, Jongebloed WL. Field emission scanning electron microscopy and transmission electron microscopy studies of the chorion, plasma membrane and syncytial layers of the gastrula-stage embryo of the zebrafish *Brachydanio rerio*: a consideration of the structural and functional relationships with respect to cryoprotectant penetration. Aquaculture Res. 2000;31:325–336.

(27). Li YY, Cheng H, Zhang ZG, Wang C, Zhu JL, Liang Y, Zhang KL, Cheng SX, Zhang XZ, Zhuo RX. Cellular internalization and *in vivo* tracking of thermosensitive luminescent micelles based on luminescent lanthanide chelate. ACS Nano 2008;2:125–133. [PubMed: 19206556]

(28). Harper S, Maddux B, Hutchison J, Usenko C, Tanguay RL. Biodistribution and toxicity of nanomaterials *in vivo*: Effects of composition, size, surface functionalization and route of exposure. Nanotech 2007;2:666–669.

(29). Chen WY, John JA, Lin CH, Chang CY. Expression pattern of metallothionein, MTF-1 nuclear translocation, and its DNA-binding activity in zebrafish (*Danio rerio*) induced by zinc and cadmium. Environ. Toxicol. Chem 2007;26:110–117. [PubMed: 17269467]

(30). Fischer HC, Liu L, Pang KS, Chan WCW. Pharmacokinetics of nanoscale quantum dots: *In vivo* distribution, sequesteration, and clearance in the rat. Adv. Funct. Mater 2006;16:1299–1305.

(31). Ballou B, Lagerholm BC, Ernst LA, Bruchez MP, Waggoner AS. Noninvasive imaging of quantum dots in mice. Bioconjug. Chem 2004;15:79–86. [PubMed: 14733586]

(32). Gao X, Cui Y, Levenson RM, Chung LW, Nie S. *In vivo* cancer targeting and imaging with semiconductor quantum dots. Nat. Biotechnol 2004;22:969–976. [PubMed: 15258594]

(33). Wiecinski PN, Metz KM, Hamers RJ, Pedersen JA. *In vitro* assay for assessing the gastrointestinal biodurability of engineered nanomaterials. Abstracts Papers Amer. Chem. Soc 2008:235–255.ENVR

(34). Aryal B, Neupane K, Sandros M, Benson D. Metallothioneins initiate semiconducting nanoparticle cellular toxicity. Small 2006;2:1159–1163. [PubMed: 17193582]

(35). Lemly AD. Teratogenic effects of selenium in natural populations of freshwater fish. Ecotoxicol. Environ Saf 1993;26:181–204. [PubMed: 7504614]

(36). Clapp AR, Medintz IL, Mauro JM, Fisher BR, Bawendi MG, Mattoussi H. Fluorescence resonance energy transfer between quantum dot donors and dye-labeled protein acceptors. J. Am. Chem. Soc 2004;126:301–310. [PubMed: 14709096]

(37). Choi AO, Cho SJ, Desbarats J, Lovric J, Maysinger D. Quantum dot-induced cell death involves Fas upregulation and lipid peroxidation in human neuroblastoma cells. J. Nanobiotechnol 2007;5:1.

(38). Heiden, TC.; Mangham, A.; Wiecinski, P.; Metz, KM.; Nesbit, D.; Pedersen, JA.; Hamers, RJ.; Heideman, W.; Peterson, RE. Surface chemistry of quantum dots affects their developmental toxicity in zebrafish. SETAC 28th Annual Meeting; Milwaukee, WI. 2007; p. 295Abstract #TRP80

(39). Hoshino A, Fujioka K, Oku T, Suga M, Sasaki YF, Ohta T, Yasuhara M, Suzuki K, Yamamoto K. Physiochemical properties and cellular toxicity of nanocrystal quantum dots depend on their surface modification. Nano Letters 2004;4:2163–2169.

(40). Arnold LJ Jr. Dagan A, Gutheil J, Kaplan NO. Antineoplastic activity of poly(L- lysine) with some ascites tumor cells. Proc. Natl. Acad. Sci U. S. A 1979;76:3246–3250. [PubMed: 291000]

(41). Takada A, Lodhi S, Weiner ND, Schacht J. Lysine and polylysine: correlation of their effects on polyphosphoinositides in vitro with ototoxic action in vivo. J. Pharm. Sci 1982;71:1410–1411. [PubMed: 6296353]

(42). Greenwald LE, Kirschner LB. The effect of poly-L-lysine, amiloride and methyl-L-lysine on gill ion transport and permeability in the rainbow trout. J. Membr. Biol 1976;26:371–383. [PubMed: 933151]

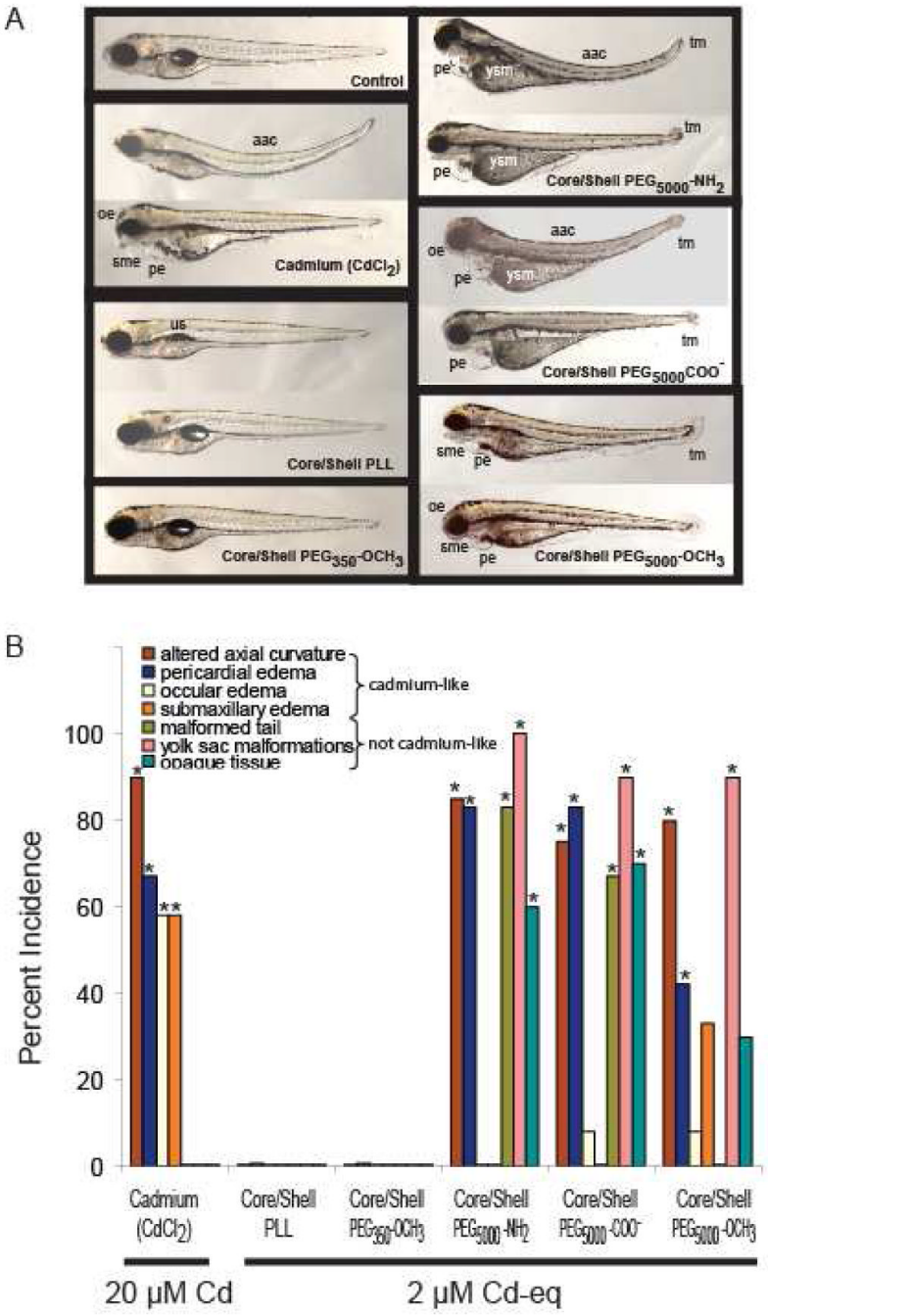

Figure 1.

A. Exposure of zebrafish larvae for 120 h to 20 µM $CdCl_2$ or 2 µM Cd equivalents of different functionalized QDs caused similar mortality (3-6%) but different endpoints of toxicity. $CdCl_2$ caused four toxic responses: altered axial curvature, pericardial edema, ocular edema, and submaxillary edema, whereas functionalized QDs caused a more complex pattern of "cadmium-like" and "not cadmium-like" responses. Endpoints of toxicity that were "not cadmium-like" consisted of: malformed tail, yolk sac malformation (yolk not absorbed), and opaque tissue indicative of tissue necrosis in the head, body, and yolk sac. This combination of "cadmium-like" and "not cadmium-like" responses to functionalized QD exposure suggested that both Cd and the functionalized QD cause toxicity. Abbreviations: aac = altered

axial curvature; sme = submandibular edema; pe = pericardial edema; yse = yolk sac edema; ysm = yolk sac malformation; oe = ocular edema; and tm = tail malformation. **B.** Effect of equally effective mortality-inducing concentrations of $CdCl_2$ (20 μM) or functionalized QDs (2 μM Cd equivalents) in zebrafish on the incidence, above that in unexposed control (not shown), of different endpoints of toxicity. Results across combined replicates ($n = 12$) are shown for exposure to 20 μM Cd (as $CdCl_2$) or to 2 μM Cd equivalents of different functionalized QDs. Asterisks denote increased incidence above unexposed control ($p < 0.05$). QD cores were CdSe and the shell was ZnS.

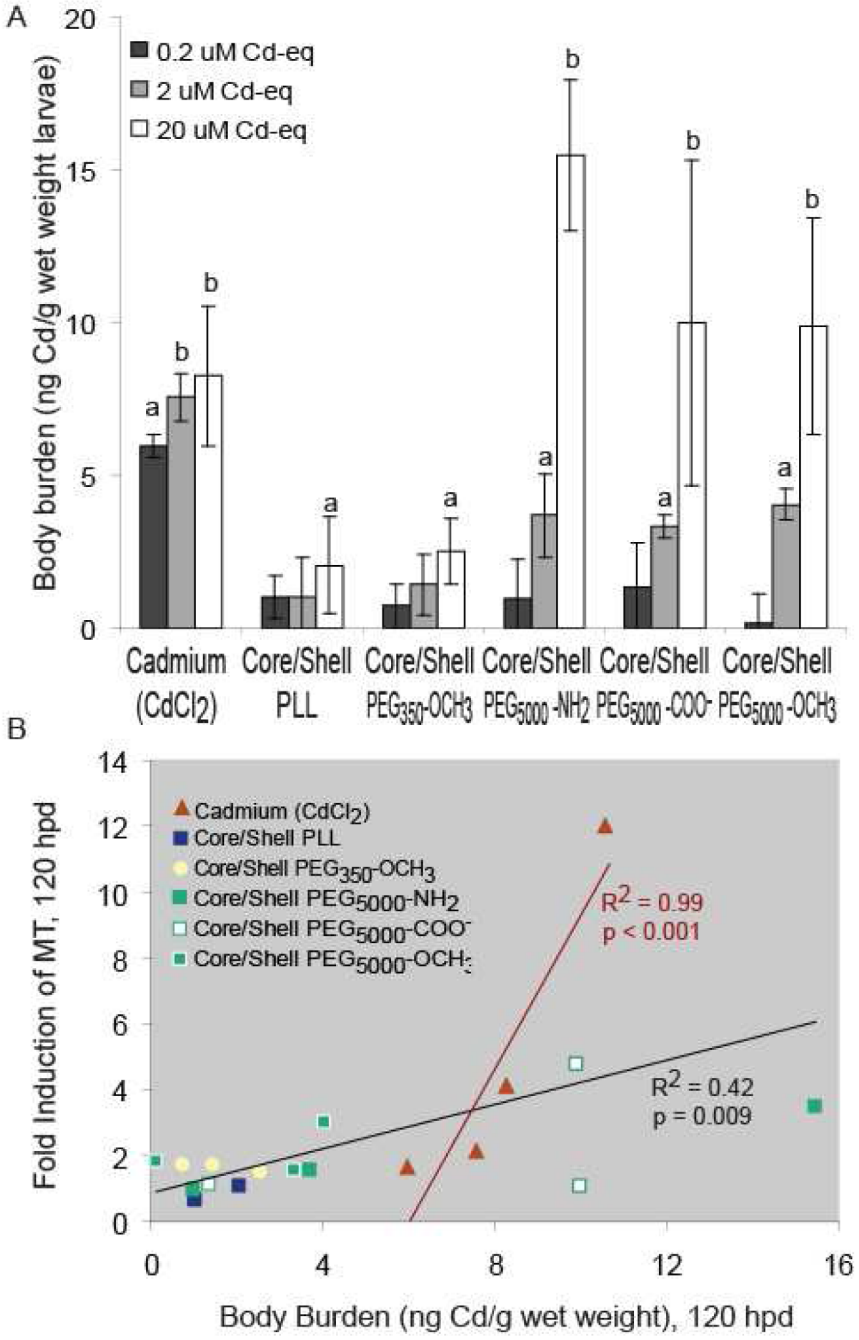

Figure 2.

A. Cadmium accumulation following 120-h waterborne exposure to graded concentrations of functionalized QDs or $CdCl_2$. The mean body burden (ng_{Cd}·glarvae^{-1}) of unexposed control Zebrafish larvae was subtracted from that of zebrafish larvae exposed to $CdCl_2$ or QDs to determine their Cd body burden. Values represent mean ± SE, n = 3 pools of 10 larvae each; letters denote significant differences ($p < 0.05$). Those without letters did not differ from unexposed control zebrafish. Insufficient numbers of embryos survived to 120 hpd to allow measurement of body burden following exposure to 200 μM Cd equivalents of QDs. **B.** Correlation between Cd body burden and MT fold induction relative mRNA abundance after 120-h exposure. $CdCl_2$ exposures (red) were correlated separately from those for QD

exposures. Correlations for individual QDs are presented in Table S1. QD cores were composed of CdSe; shells were ZnS.

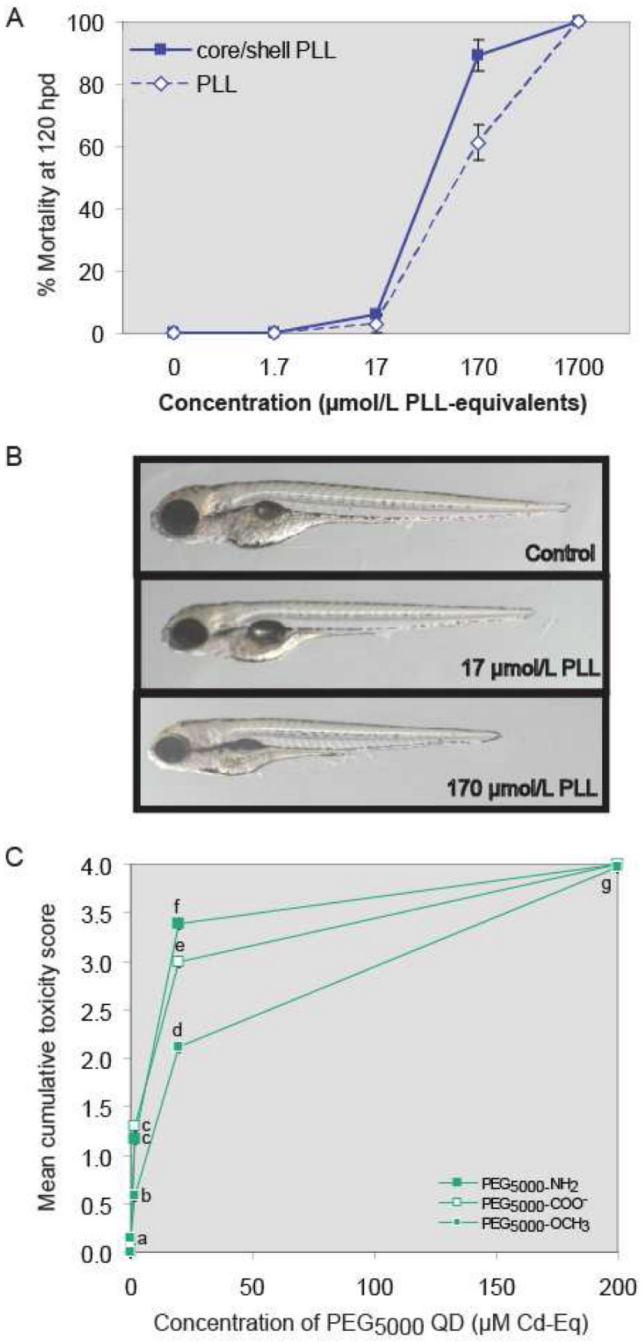

Figure 3.

A. Comparison of mortality induced by PLL-wrapped $CdSe_{core}/ZnS_{shell}$ QDs with that produced by PLL alone. Expressed as PLL equivalents, LC_{50} values for $CdSe_{core}/ZnS_{shell}$-PLL QDs and PLL were 59 (44-75) and 125 (95-154) µM (95% confidence intervals in parentheses). **B.** Representative photomicrographs of larvae exposed to PLL alone. Beyond reduced growth, no sublethal toxicity was seen. **C.** Cumulative toxicity scores following 120-h exposure to $CdSe_{core}/ZnS_{shell}$ PEG_{5000} QDs with different surface chemistries. Values represent mean ± SE ($n = 36$); letters denote significant differences ($p < 0.05$). Note: Error bars are present, but smaller than symbols used in the graph.

Table 1

Physicochemical Properties and LC_{50} Values in Zebrafish Larvae for Functionalized Quantum Dots[a,b]

Toxicant	d_{core} (nm)	d_{calc} (nm)	EM, 28°C			LC_{50} After 120-h Exposure	
			$d_{h,n}$ (nm)	ζ-Potential (mV)	Max. Cd release (μM)	μM Cd-eq	#QD 100μL^{-1}
$CdSe_{core}/ZnS_{shell}$-PLL	3.2	9	382 ± 8	3.0 ± 1.0	38 ± 8.6	7 (6-9)	10×10^{11}
$CdSe_{core}/ZnS_{shell}$-PEG_{350}-OCH_3	2.6	7	600 ± 30	8.0 ± 0.5	4 ± 0.4	-----	-----
$CdSe_{core}/ZnS_{shell}$-PEG_{5000}-NH_2	2.6	14	23 ± 1	-2.0 ± 0.2	10 ± 1.2	21 (17-27)	7×10^{12}
$CdSe_{core}/ZnS_{shell}$-PEG_{5000}-COO^-	2.6	14	44 ± 8	-5.0 ± 0.4	2 ± 1.4	28 (13-63)	10×10^{12}
$CdSe_{core}/ZnS_{shell}$-PEG_{5000}-OCH_3	2.6	14	21 ± 1	-2.0 ± 0.6	28 ± 1.2	42 (24-75)	15×10^{12}
$CdCl_2$	-----	-----	-----	-----	-----	409 (270-563)	-----

[a] LC_{50} values are reported as the concentration of QDs expressed as cadmium-equivalents (μM Cd-eq) and numbers of QDs (#QD) suspended in 100μL exposure medium. The 95% confidence interval for each LC_{50} is shown in parentheses. LC_{50} of $CdCl_2$ shown for comparison.

[b] Abbreviations: d_{core}, diameter of $CdSe_{core}$ determined by UV-Visible spectroscopy; d_{calc}, calculated diameter of QD (accounting for CdSe core diameter, ZnS shell thickness, and organic coating thickness. For PEG ligands, the poly(ethylene glycol) chain was assumed to be fully extended. See SI for detailed methods.); $d_{h,n}$, number-average hydrodynamic diameter; EM, embryo medium (58 mM $CaCl_2$, 0.7 mM KCl, 0.4 mM $MgSO_4 \cdot 7H_2O$, 0.6 mM $Ca(NO_3)_2 \cdot 4H_2O$, 0.5 mM HEPES, pH 7, I = 0.18 M); PEG, polyethylene glycol; PLL, poly-L-lysine.